

Supporting Information for

ORIGINAL ARTICLE

Macrophage-mediated tumor-targeted delivery of engineered *Salmonella typhimurium* VNP20009 in anti-PD1 therapy against melanoma

Leyang Wu^{a,b,†}, Lin Li^{a,†}, Shufeng Li^{d,†}, Lina Liu^a, Wenjie Xin^a, Chenyang Li^a, Xingpeng Yin^a, Xuebo Xu^a, Feifei Bao^a, Zichun Hua^{a,b,c,*}

^a*The State Key Laboratory of Pharmaceutical Biotechnology, School of Life Sciences, Nanjing University, Nanjing 210023, China*

^b*Changzhou High-Tech Research Institute of Nanjing University and Jiangsu TargetPharma Laboratories Inc., Changzhou 213164, China*

^c*School of Biopharmacy, China Pharmaceutical University, Nanjing 210023, China*

^d*Key Laboratory of Developmental Genes and Human Disease in Ministry of Education, Department of Biochemistry and Molecular Biology, Medical School of Southeast University, Nanjing 210009, China*

Received 26 January 2022; received in revised form 7 April 2022; accepted 25 April 2022

*Corresponding author. Tel.: +86 025 83324605.

E-mail address: zchua@nju.edu.cn (Zichun Hua).

[†]These authors made equal contributions to this work.

Running title: Triple combination immunotherapy against melanoma

Supporting Figures S1–S26

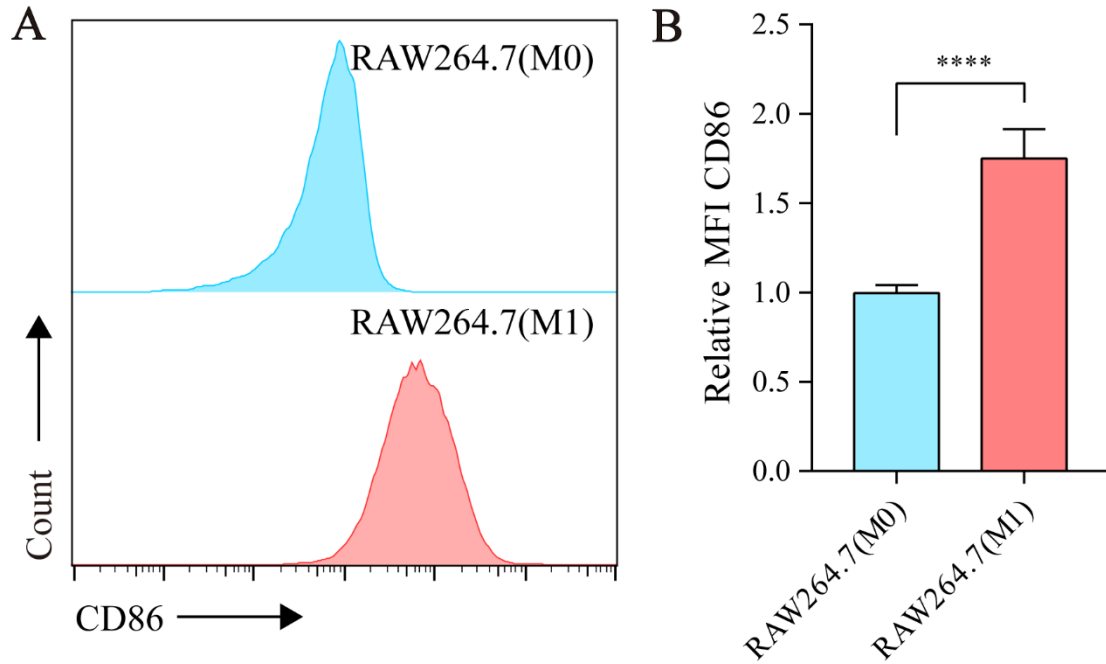


Figure S1 RAW264.7 cells were polarized to the M1 type after LPS stimulation. Changes in cell surface CD86 were detected after treatment of RAW264.7 (M0) cells with 100 ng/mL LPS for 12 h ($n = 3$). A representative flow cytometry plot is shown in (A), and the results are shown as a bar plot in (B). Data in (B) are reported as the mean \pm SEM. All data are representative of three independent experiments. Statistics were calculated using the two-tailed, unpaired Student's t test with Welch's correction. **** $P \leq 0.0001$.

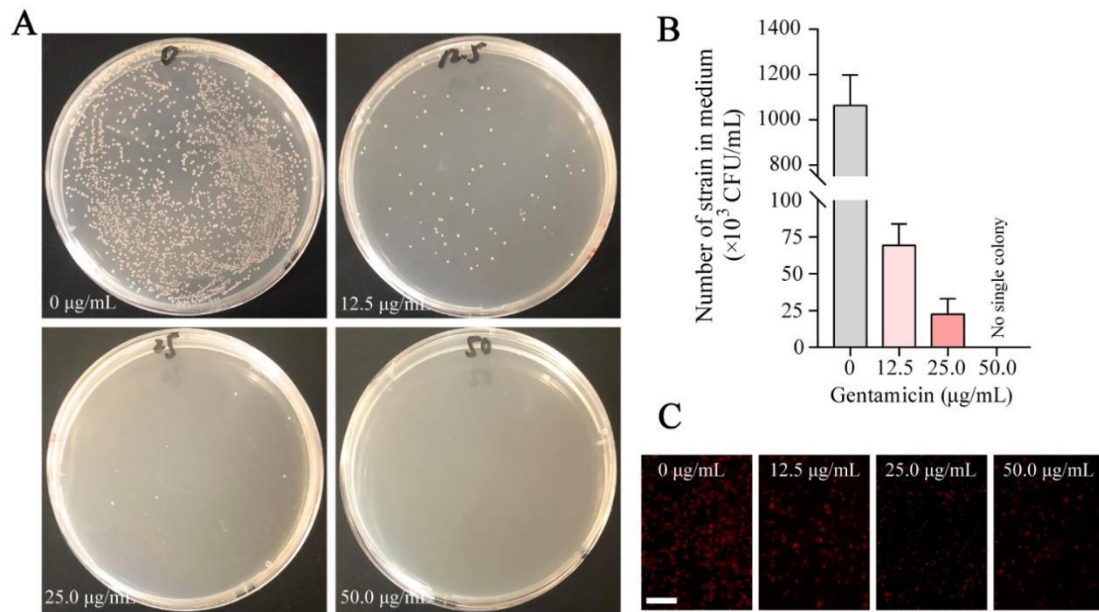


Figure S2 Gentamicin (50 $\mu\text{g/mL}$) completely eliminated the VNP within 60 min. VNP-RFP (5×10^5 CFU) was inoculated with 1 mL of DMEM supplemented with different concentrations of gentamicin (0/12.5/25/50 $\mu\text{g/mL}$) and incubated in a 37 $^\circ\text{C}$ incubator for 60 min. The different groups of media were diluted 100-fold, and 100 μL was spread on LB agar plates with kanamycin ($n = 3$). Representative images of plates are shown in (A). (B) Number of bacteria in the medium calculated from the number of single colonies on the plates. (C) Fluorescence images of VNP-RFP after 60 min of treatment with different concentrations of gentamicin (Scale bar = 50 μm). Data in (B) are reported as the mean \pm SEM. All data are representative of three independent experiments.

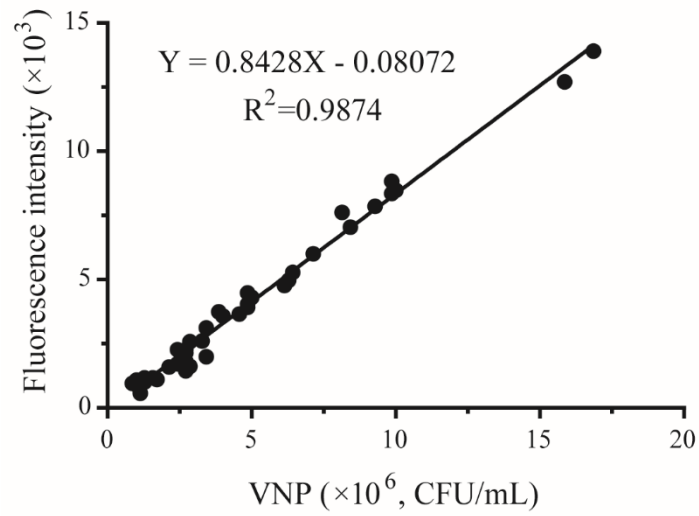


Figure S3 Correlation between the VNP-RFP fluorescence intensity and bacterial counts. Correlation and linear regression analyses were performed in GraphPad Prism using Pearson's correlation coefficients.

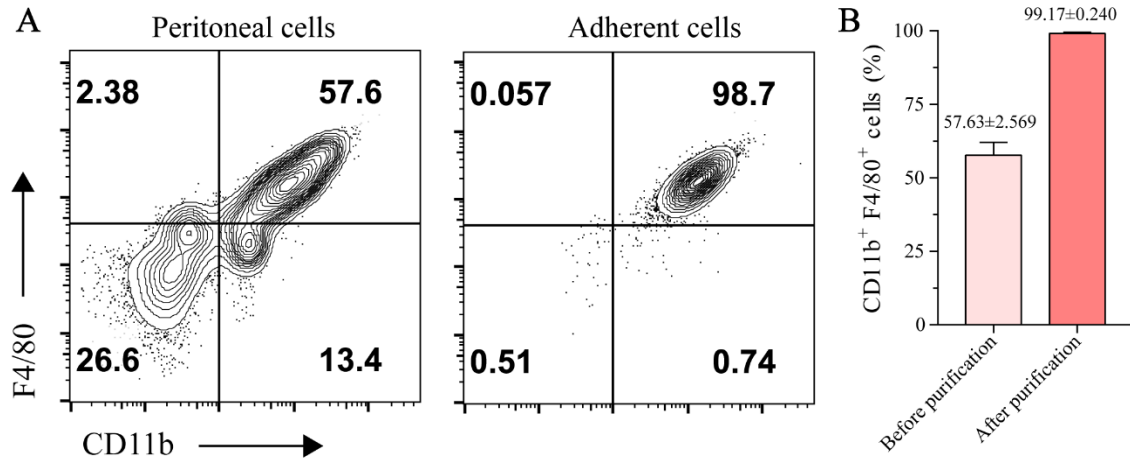


Figure S4 High-purity peritoneal macrophages were stably obtained by adherent isolation from peritoneal cells. The purity of peritoneal macrophages (PEM Φ), which were obtained by starch broth stimulus and adherent separation, was analyzed by flow cytometry. (A) Representative FACS analysis of macrophage purity before and after purification. (B) Quantification analysis of the percent of macrophages in (A) ($n = 3$). Data in (B) are reported as the mean \pm SEM. All data are representative of three independent experiments.

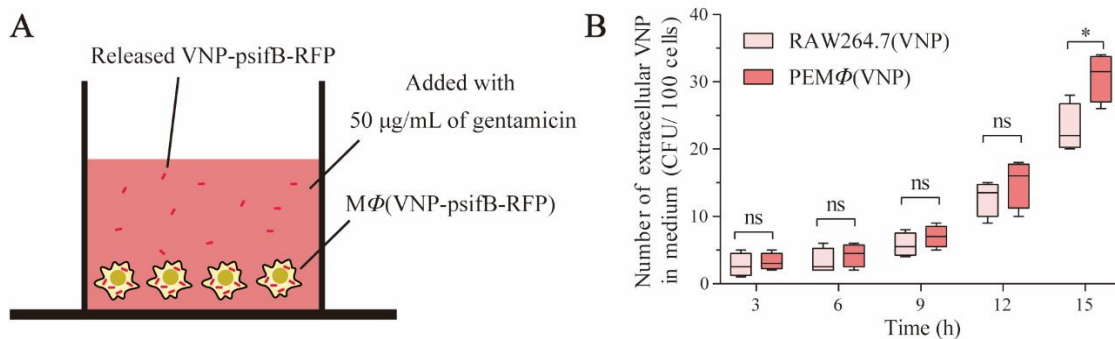


Figure S5 The VNP strain was slowly released from macrophages. (A) The prepared RAW264.7(VNP- ψ sifB-RFP) cells and PEM Φ (VNP- ψ sifB-RFP) cells were incubated in medium supplemented with 50 μ g/mL gentamicin to kill released extracellular bacteria while not affecting the visualization of strains according to Fig. S2C. The released bacteria were observed and recorded with a microscope at different times. (B) The number of VNP in the microscopic field in (A) was recorded at different time points (3–15 hours), and the average number of bacteria per 100 cells was calculated ($n = 4$). Boxplot representations of the spot counts. The median, interquartile range, and minimum and maximum identifiers are shown. All data are representative of two independent experiments. Statistics were calculated using the two-tailed, unpaired Student's t test with Welch's correction. n.s. = not significant, $*P \leq 0.05$.

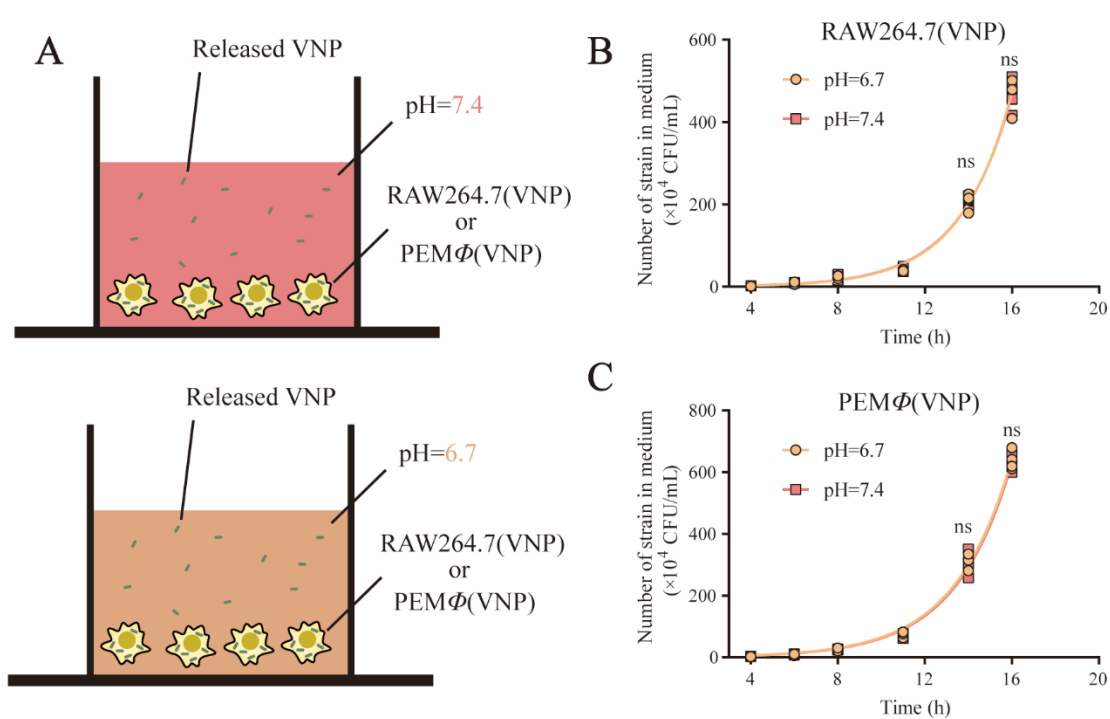


Figure S6 Weakly acidic environment had no significant effect on the release of strains and their proliferation. (A) The prepared RAW264.7(VNP) and PEM Φ (VNP) cells were incubated in medium with different pH values (7.4 and 6.7) adjusted by dilute hydrochloric acid to release intracellular VNP, and the medium was collected at different times for subsequent experiments. (B) The correlation between the number of VNP strains released from RAW264.7(VNP) cells and the culture time in (A) was analyzed ($n = 4$). (C) The correlation between the number of VNP strains released from PEM Φ (VNP) cells and the culture time in (A) was analyzed ($n = 4$). All data are representative of two independent experiments. Statistics were calculated using the two-tailed, unpaired Student's t test with Welch's correction. n.s. = not significant.

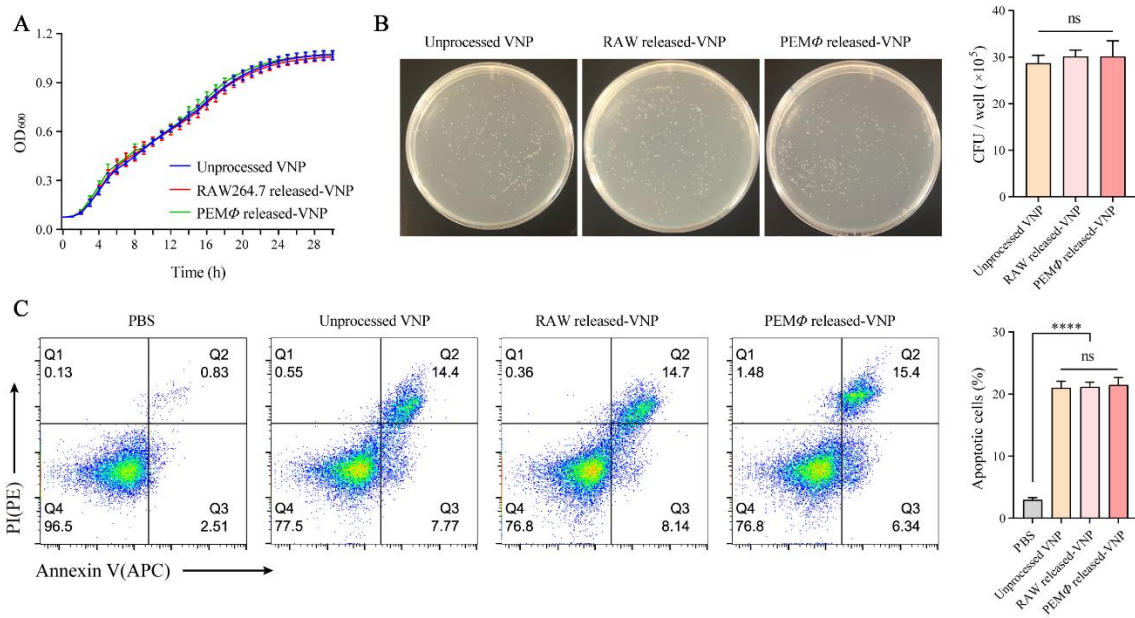


Figure S7. VNP released from macrophages was similar to unprocessed VNP in terms of the bacterial growth rate, and invasion and killing ability on tumor cells. (A) Growth curves of unprocessed VNP, RAW264.7 released-VNP and PEMΦ released-VNP in LB at 37 °C ($n = 4$). (B) B16F10 cells were infected with different VNP at a MOI of 100 for 1 h. After infection, the cells were washed with PBS and then treated with 50 $\mu\text{g}/\text{mL}$ gentamicin for 1 h to remove residual VNP. Cells were lysed with 0.5% Triton X-100, and the number of internalized VNP was determined by plating 10,000-fold dilutions of the cell lysates on LB plates ($n = 5$). (C) Representative FACS analysis of Annexin V and propidium iodide (PI) staining after B16F10 cells were incubated with different strains at a MOI of 100 for 4 h, and the quantification analysis of the percent of apoptotic cells (Annexin V⁺ cells) is shown on the right ($n = 3$). Data are reported as the mean \pm SEM. All data are representative of two independent experiments. Statistics were calculated using the two-tailed, unpaired Student's t test with Welch's correction. n.s. = not significant, **** $P \leq 0.0001$.

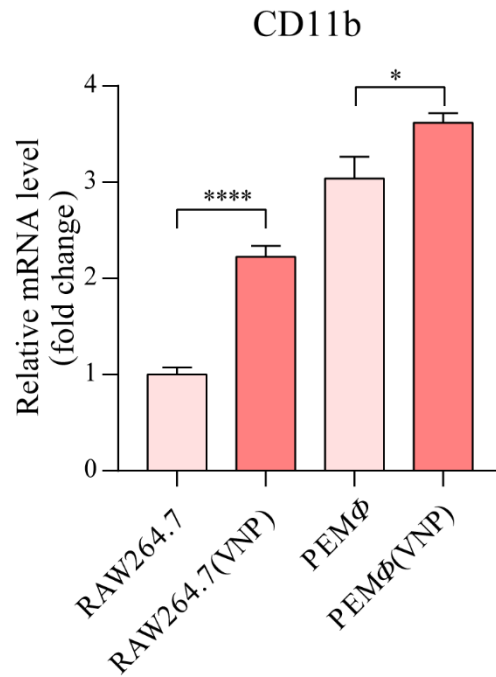


Figure S8 CD11b mRNA expression levels in RAW264.7/RAW264.7(VNP) and PEM ϕ /PEM ϕ (VNP) cells. Data are reported as the mean \pm SEM. All data are representative of two independent experiments. Statistics were calculated using the two-tailed, unpaired Student's *t* test with Welch's correction. * $P \leq 0.05$, **** $P \leq 0.0001$.

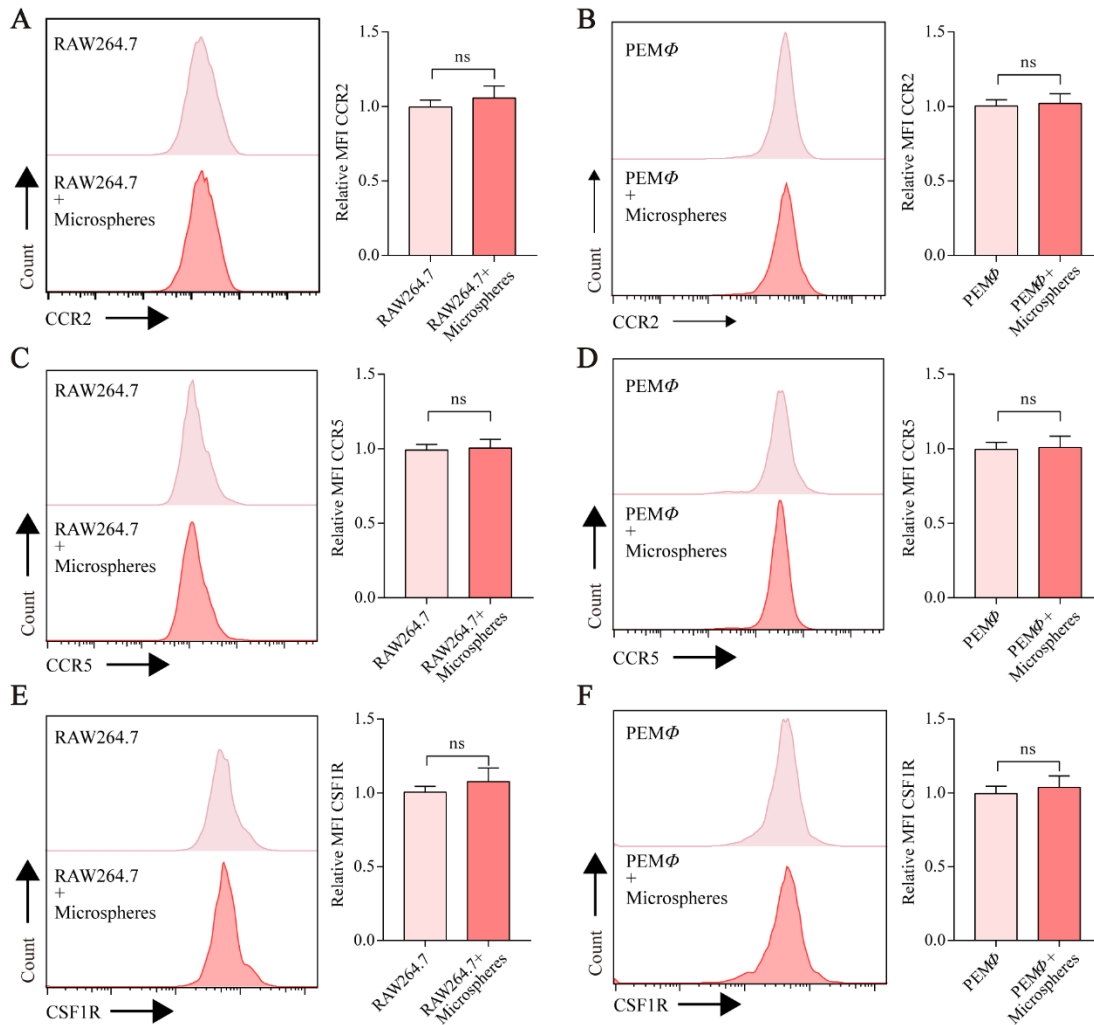


Figure S9 Surface membrane protein levels of macrophages were not significantly altered by phagocytosis. RAW264.7 and PEM ϕ cells were mixed with fluorescence microspheres at a ratio of 1:10 and incubated at 37 °C for 1 h, similar to the process of loading VNP. After removing the microspheres and continuing the incubation for 1 h, the cells were collected to compare the quantity changes in membrane protein by flow cytometry. Comparison of cell surface (A, B) CCR2, (C, D) CCR5 and (E, F) CSF1R after RAW264.7/PEM ϕ cells were incubated with or without the addition of fluorescent microspheres ($n = 3$ in all data). Data are reported as the mean \pm SEM. All data are representative of two independent experiments. Statistics were calculated using the two-tailed, unpaired Student's t test with Welch's correction. n.s. = not significant.

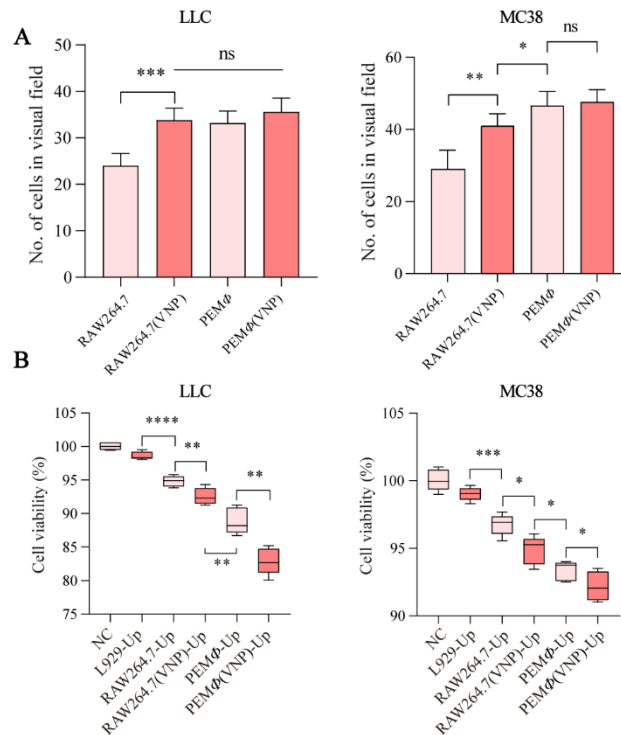


Figure S10 VNP-loaded macrophages maintain high tumor chemotaxis and achieve higher tumoricidal activity. (A) Transwell migration assay of RAW264.7/RAW264.7(VNP) and PEMΦ/PEMΦ(VNP) cells toward LLC and MC38 tumor cells (coculture for 16 h and added with 50 μg/mL gentamicin). The experiment shares the same blank group as that in Fig. 2D. (B) The prepared cells and tumor cells were cocultured as shown in Fig. 2E, and the proliferation of LLC and MC38 tumor cells was examined by CCK-8 assays ($n = 4$ in all data). Data are reported as the mean \pm SEM. Boxplot representations of the spot counts. The median, interquartile range, and minimum and maximum identifiers are shown. All data are representative of two independent experiments. Statistics were calculated using the two-tailed, unpaired Student's t test with Welch's correction. n.s. = not significant, $*P \leq 0.05$, $**P \leq 0.01$, $***P \leq 0.001$, $****P \leq 0.0001$.

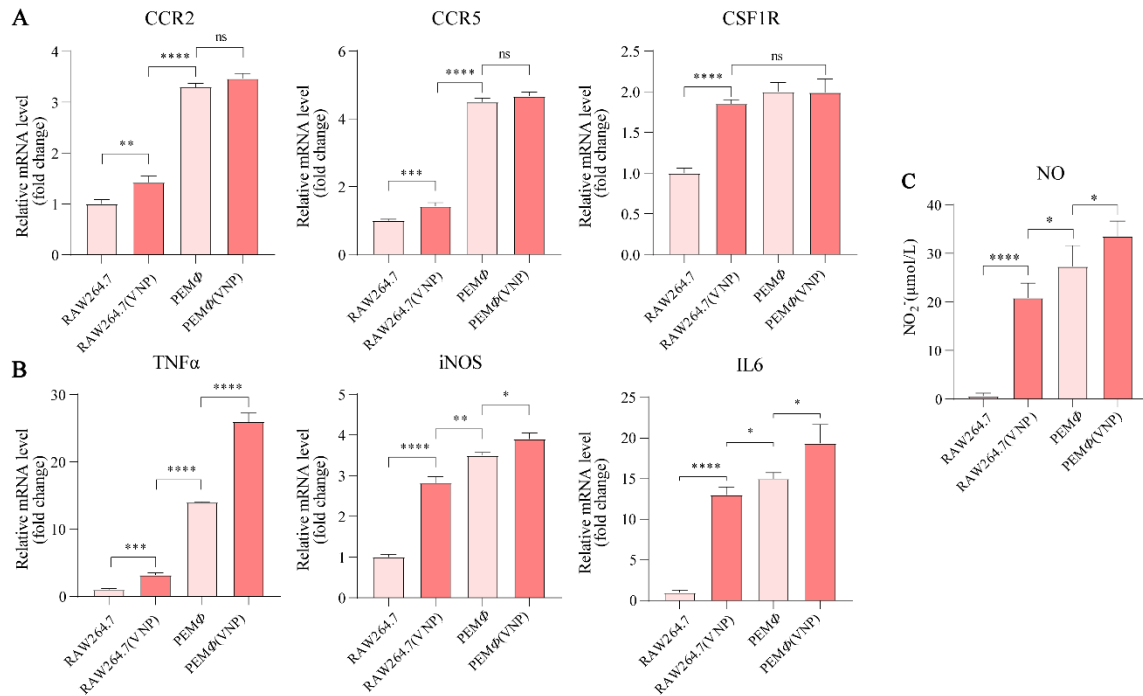


Figure S11 VNP loading enhances cytokine expression, chemokine receptor expression, and cytotoxicity in macrophages. (A) CCR2, CCR5 and CSF1R chemokine receptor mRNA expression levels in RAW264.7/RAW264.7 (VNP) and PEMΦ/PEMΦ(VNP) cells. (B) TNFα, iNOS and IL6 mRNA expression levels in RAW264.7/RAW264.7 (VNP) and PEMΦ/PEMΦ(VNP) cells. (C) Analysis of intracellular NO in RAW264.7/RAW264.7 (VNP) and PEMΦ/PEMΦ(VNP) cells ($n = 3$ in all data). Data are reported as the mean \pm SEM. All data are representative of two independent experiments. Statistics were calculated using the two-tailed, unpaired Student's t test with Welch's correction. n.s. = not significant, * $P \leq 0.05$, ** $P \leq 0.01$, *** $P \leq 0.001$, **** $P \leq 0.0001$.

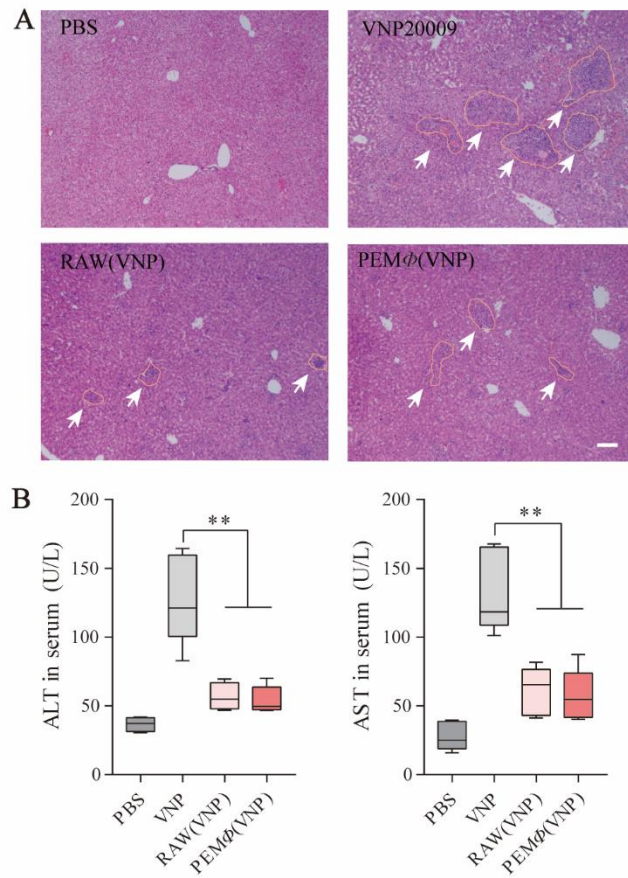


Figure S12 VNP-loaded macrophages effectively attenuate VNP-induced liver damage. (A) A close-up view of representative H&E staining showing liver injury (white arrow) 1 day after treatment (Scale bar = 100 μ m). (B) Serum alanine transaminase (ALT) and aspartate transaminase (AST) levels 1 day after different treatments ($n = 5$ mice per group). Data in (B) are reported as the mean \pm SEM. Statistics were calculated using the two-tailed, unpaired Student's t test with Welch's correction. $**P \leq 0.01$.

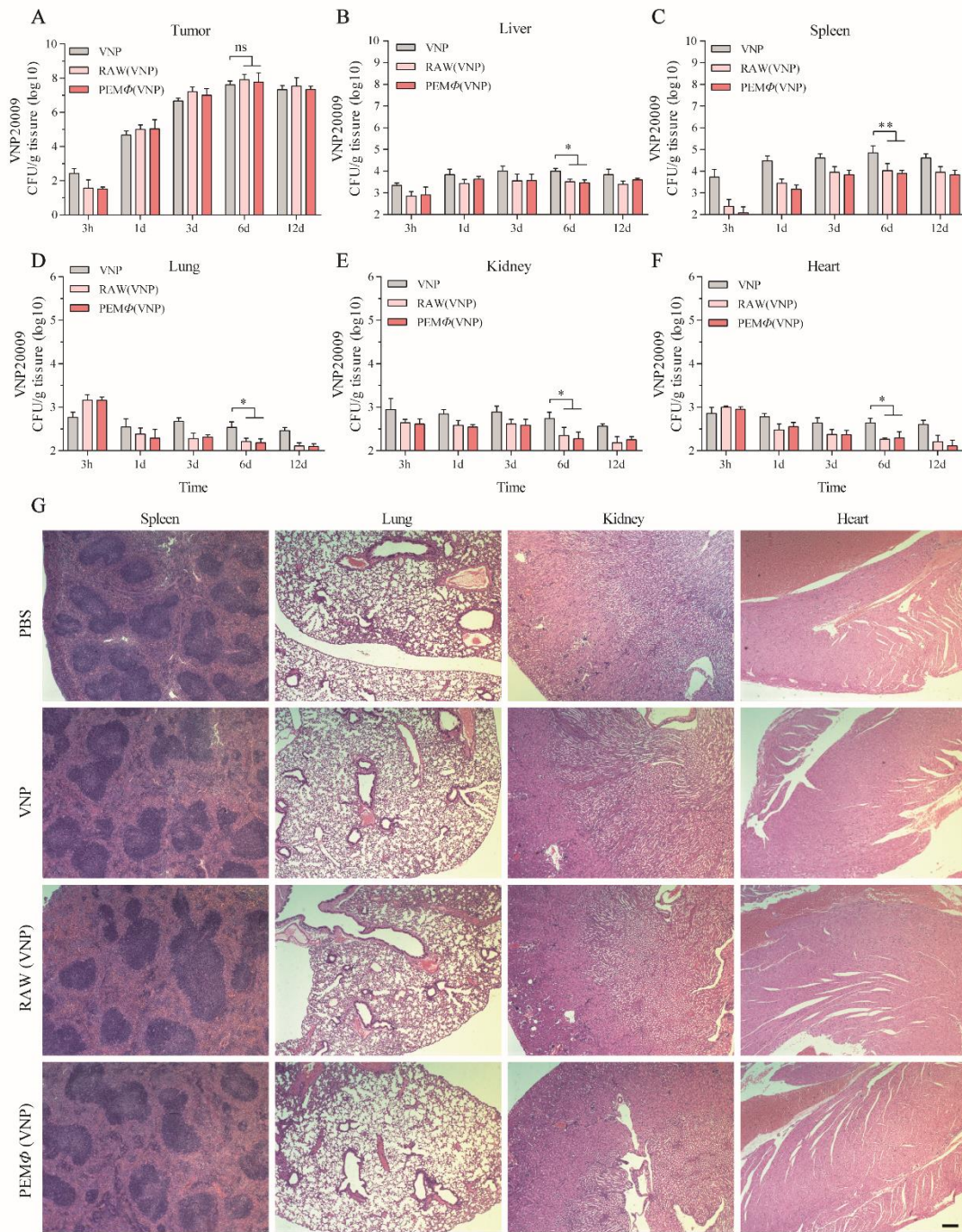


Figure S13 VNP loading into macrophages reduces the off-target effects of VNP. (A–F) The VNP titers in the tumor, liver, spleen, lung, kidney and heart were determined at specific time points after the administration of VNP, RAW(VNP) and PEM ϕ (VNP) cells

($n = 4$ or 5 mice per group). (G) A close-up view of representative H&E staining of spleen, lung, kidney and heart sections (Scale bar = $40\ \mu\text{m}$). Data in (A–F) are reported as the mean \pm SEM. All data are representative of two independent experiments. Statistics were calculated using the two-tailed, unpaired Student's t test with Welch's correction. n.s. = not significant, $*P \leq 0.05$, $**P \leq 0.01$.

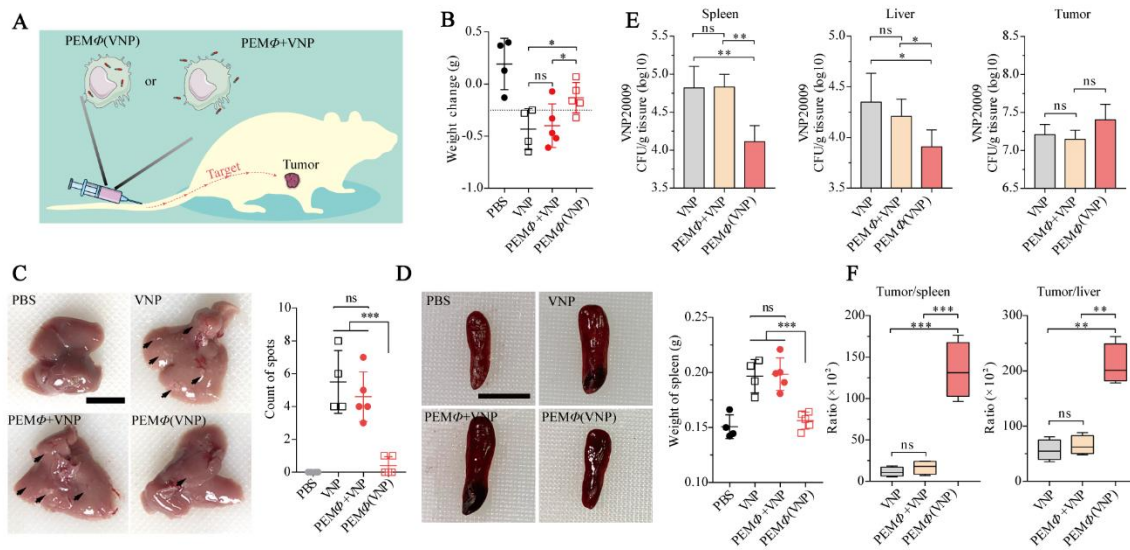


Figure S14 Treatment with a mixture of PEM ϕ cells and VNP failed to reduce the toxicity of VNP. (A) VNP-loaded PEM ϕ (PEM ϕ (VNP)) cells and a mixture of PEM ϕ and VNP (PEM ϕ +VNP) were administered *via* the tail vein, and their toxicities and tumor targeting were evaluated ($n = 4$ or 5 mice per group). (B) Changes in body weight 1 day after administration. (C) Photographs of representative livers. The black arrows indicate the pathological spots on the livers, and the numbers of spots are plotted in the chart (Scale bar = 10 mm). (D) Photographs of representative spleens. The weights of the spleens in each group are plotted in the chart (Scale bar = 10 mm). (E, F) Quantification of VNP titers in the tumor, spleen, and liver (E) and the ratio of the VNP titer in the tumor and spleen or tumor and liver (F) in each group on Day 6 ($n = 5$ mice per group). Data in (C), (D) and (E) are reported as the mean \pm SEM. Boxplot representations of the spot counts. The median, interquartile range, and minimum and maximum identifiers are shown. All data are representative of two independent experiments. Statistics were calculated using the two-tailed, unpaired Student's *t* test with Welch's correction. n.s. = not significant, * $P \leq 0.05$, ** $P \leq 0.01$, *** $P \leq 0.001$.

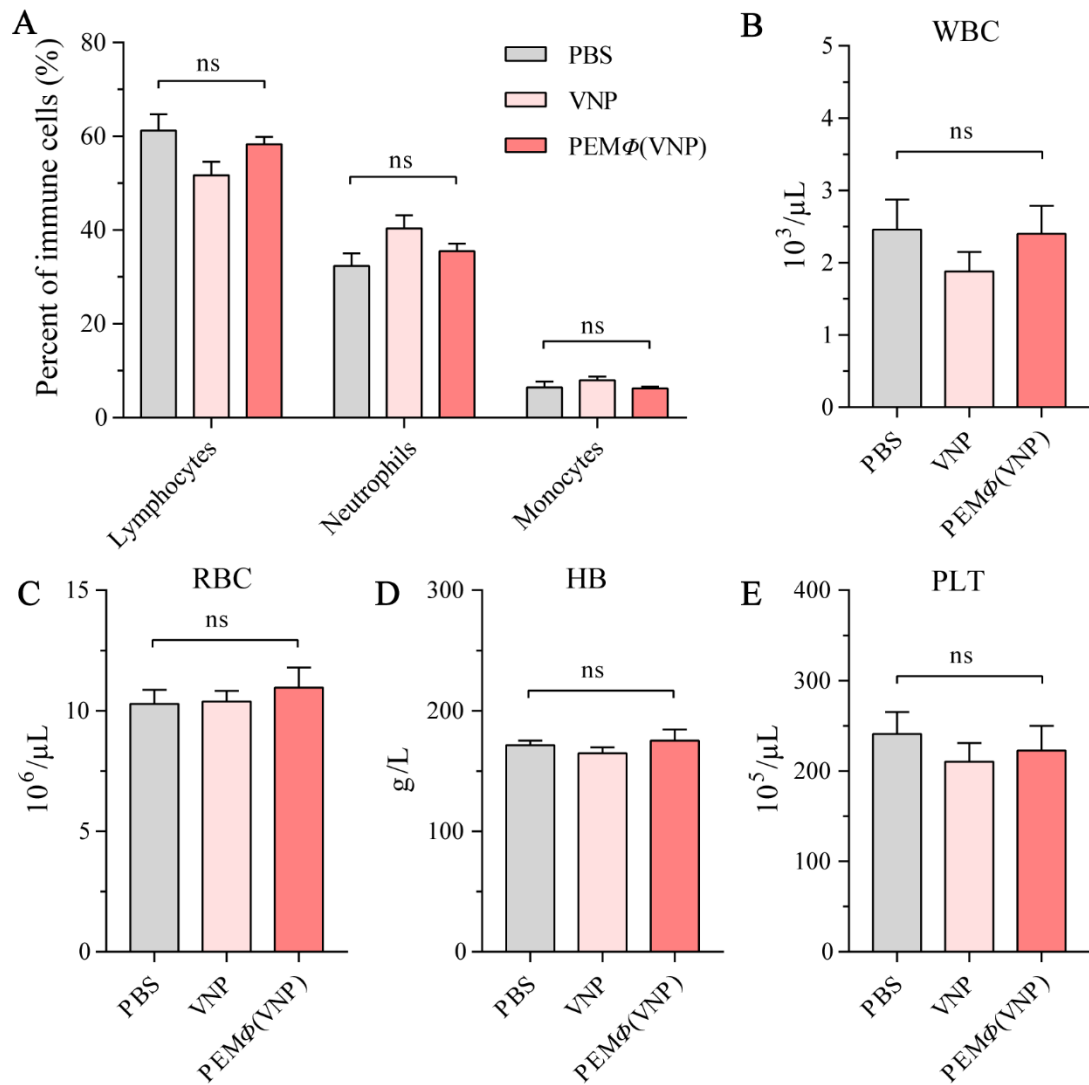


Figure S15 Routine blood parameters of the mice. (A–E) Comprehensive hematology of blood drawn from B16F10 tumor-bearing mice 1 day after intravenous injection with PBS, VNP strains or PEM ϕ (VNP) cells ($n = 5$ mice per group). PEM ϕ (VNP) cells had no significant effect on the percentage of mainly immune cells or the levels of white blood cells (WBC), red blood cells (RBC), hemoglobin (HB), and platelets (PLT) in mice. Data are reported as the mean \pm SEM. All data are representative of two independent experiments. Statistics were calculated using the two-tailed, unpaired Student's t test with Welch's correction. n.s. = not significant.

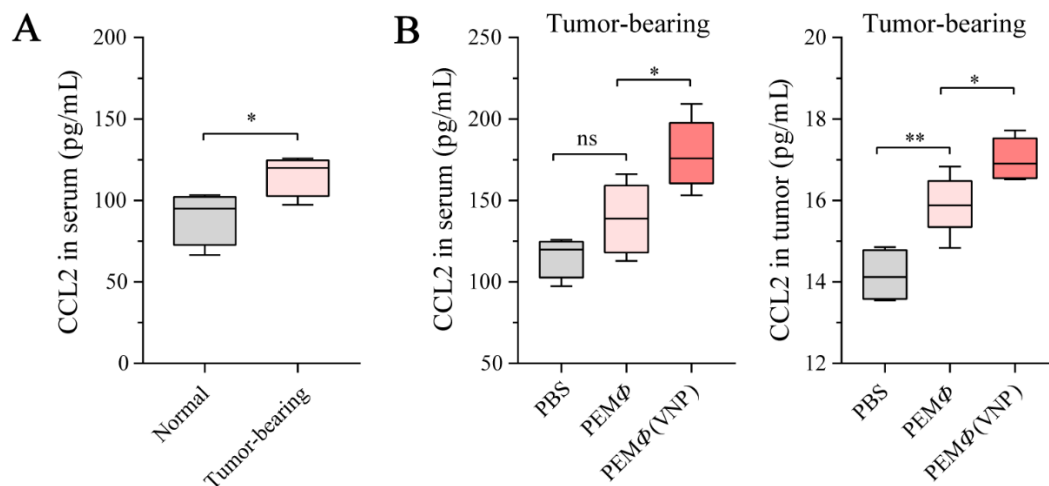


Figure S16 Detection of serum and tumor CCL2 levels in B16F10 tumor-bearing mice. (A) Detection of CCL2 concentration in peripheral blood of normal mice and B16F10 tumor-bearing mice (tumor size = 100 mm³, $n = 4$ mice per group). (B) Detection of CCL2 concentration in peripheral blood of B16F10 tumor-bearing mice (tumor size = 100 mm³) 24 h after administration ($n = 4$ or 5 mice per group). Boxplot representations of the spot counts, with the median, interquartile range, and minimum and maximum identifiers, are shown. The experiment was performed once. Statistics were calculated using the two-tailed, unpaired Student's t test with Welch's correction. n.s. = not significant, $*P \leq 0.05$, $**P \leq 0.01$.

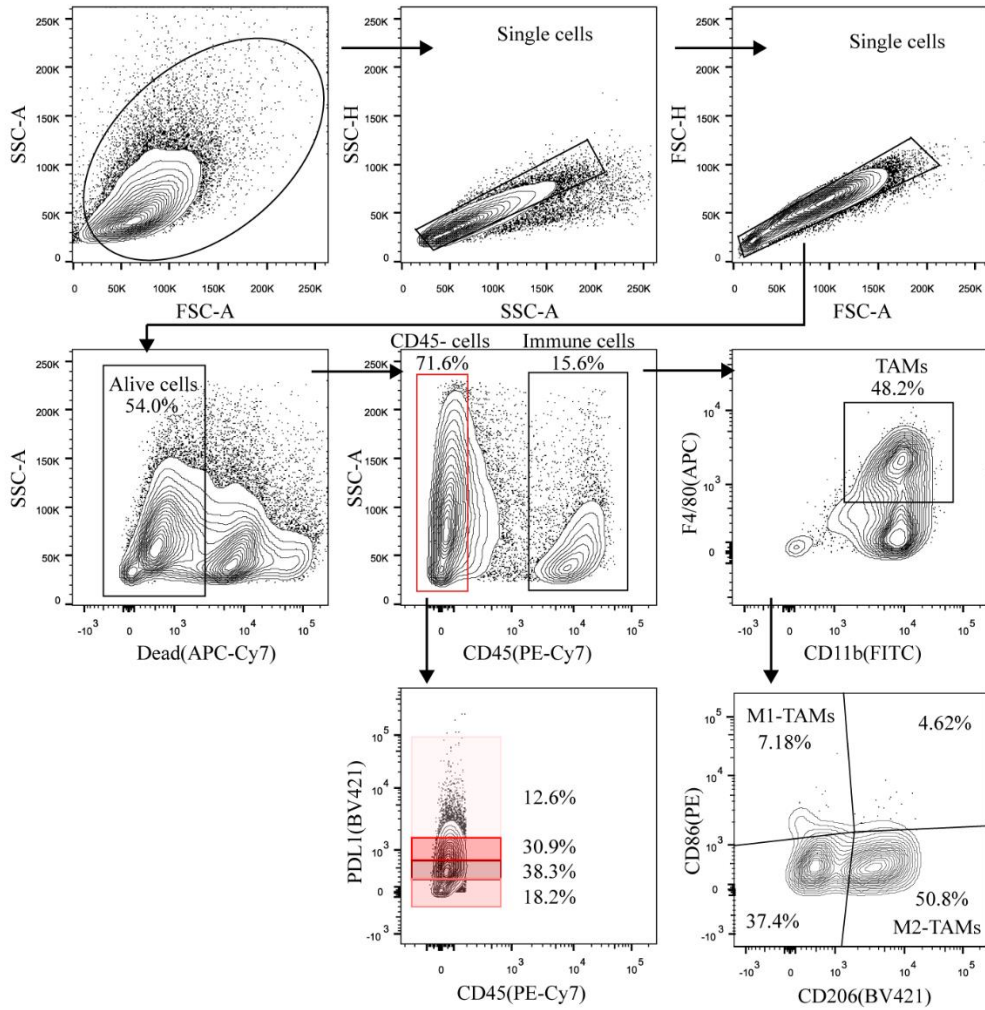


Figure S17 Representative gating strategy to identify tumor cells with different expression levels of PDL1 and M1-like/M2-like (tumor-associated macrophages) TAMs.

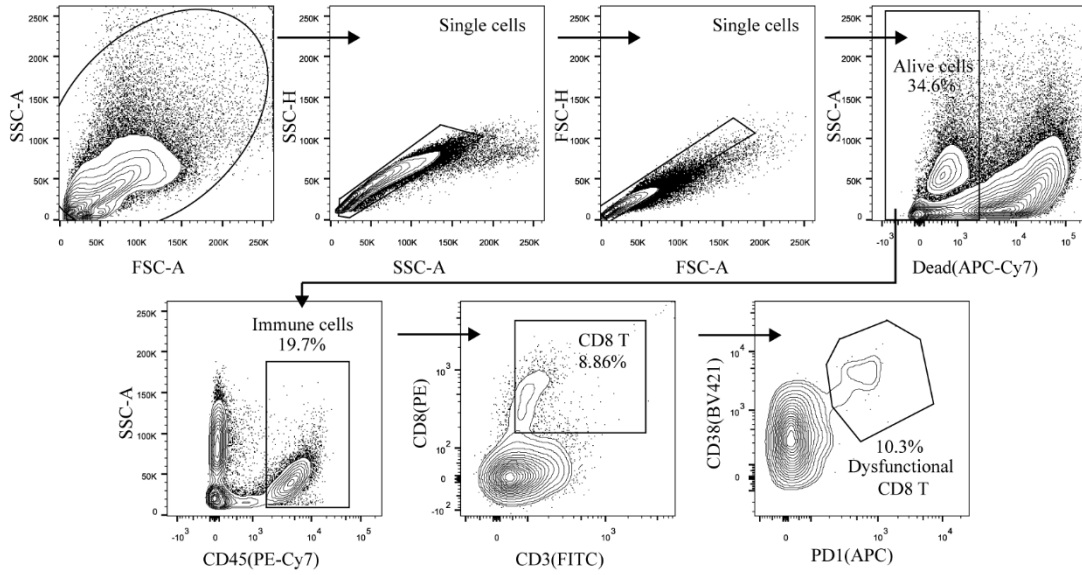


Figure S18 Representative gating strategy for CD8⁺ T cell dysfunction analysis.

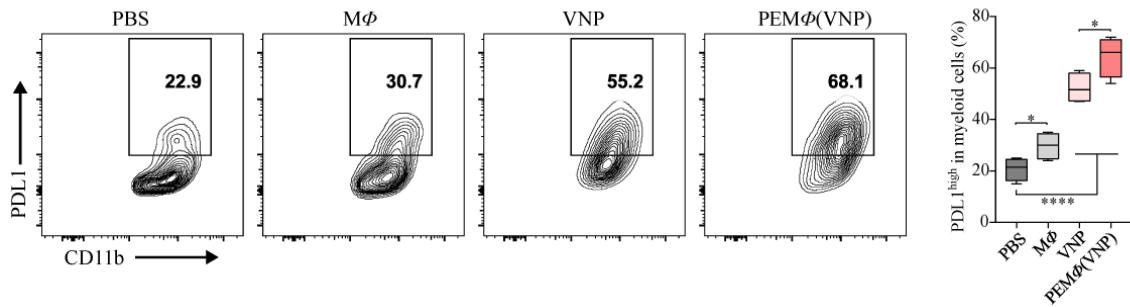


Figure S19 Proportion of PDL1 on the surface of tumor-associated myeloid cells after the administration of PBS, PEM ϕ , VNP or PEM ϕ (VNP) cells on Day 3 ($n = 4$ mice per group). Boxplot representations of the spot counts. The median, interquartile range, and minimum and maximum identifiers are shown. The data are representative of two independent experiments. Statistics were calculated using the two-tailed, unpaired Student's t test with Welch's correction. n.s. = not significant, * $P \leq 0.05$, ** $P \leq 0.01$, *** $P \leq 0.001$.

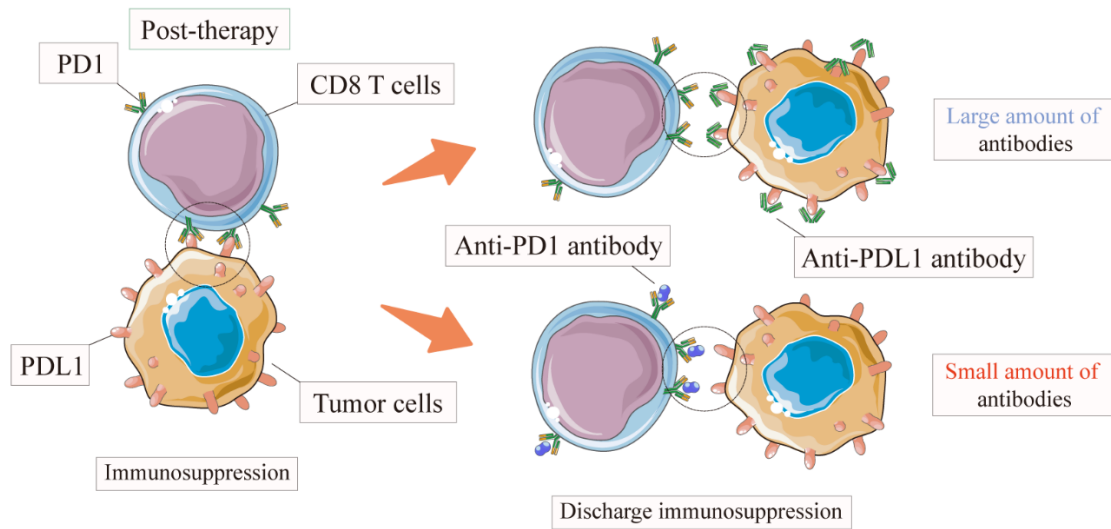


Figure S20 Schematic diagram of reverse immunosuppression after treatment with different types of antibodies, including anti-PD1/PDL1 antibody. Compared with the use of anti-PDL1 antibody to block PDL1 on the surface of innumerable tumor cells, only a lower dose of anti-PD1 antibody is required to achieve reverse immunosuppression between T cells and tumor cells by blocking PD1 on the surface of T cells.

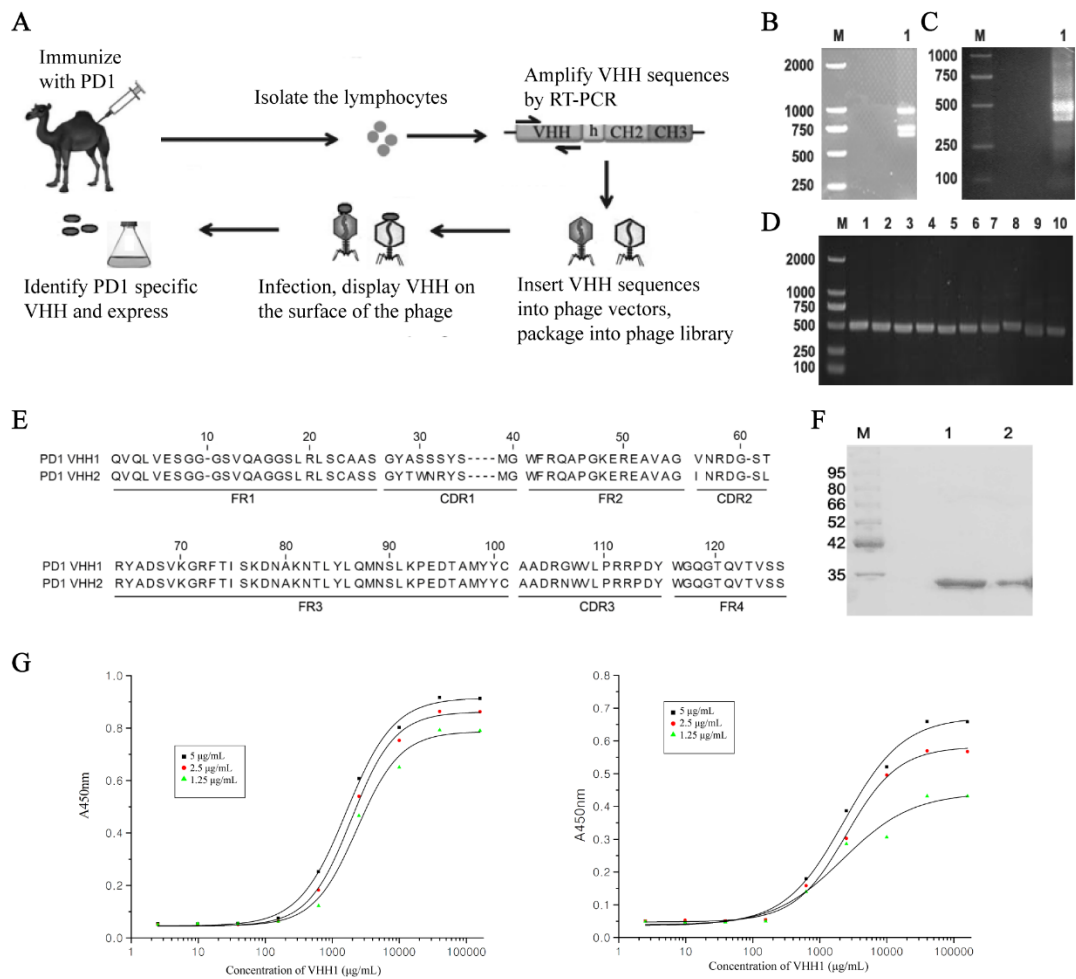


Figure S21 Construction and characterization of anti-PD1 nanoantibodies. (A) Scheme showing PD1 VHH library construction. (B) The first round nest-PCR fragments had evident bands at approximately 900 and 700 bp. M: marker; 1: nest-PCR product. (C) VHH genes of approximately 500 bp were amplified by a second PCR, M: marker; 1: nest-PCR product. (D) Ten plaques were randomly selected to detect the percentage of phage containing an insert of VHH. (E) Alignment of the amino acid sequence of the PD1-specific binding nanobodies named VHH1 and VHH2. (F) Purified soluble nanobodies were analyzed by SDS-PAGE. Lane 1: VHH1, Lane 2: VHH2. (G) The affinity of Nbs for PD1 was determined by noncompetitive ELISA. The plates were coated with PD1 protein at three concentrations: 5, 2.5 and 1.25 µg/mL. Experimental dose-response curves for anti-PD1 VHHs at three different PD1 coating concentrations were plotted.

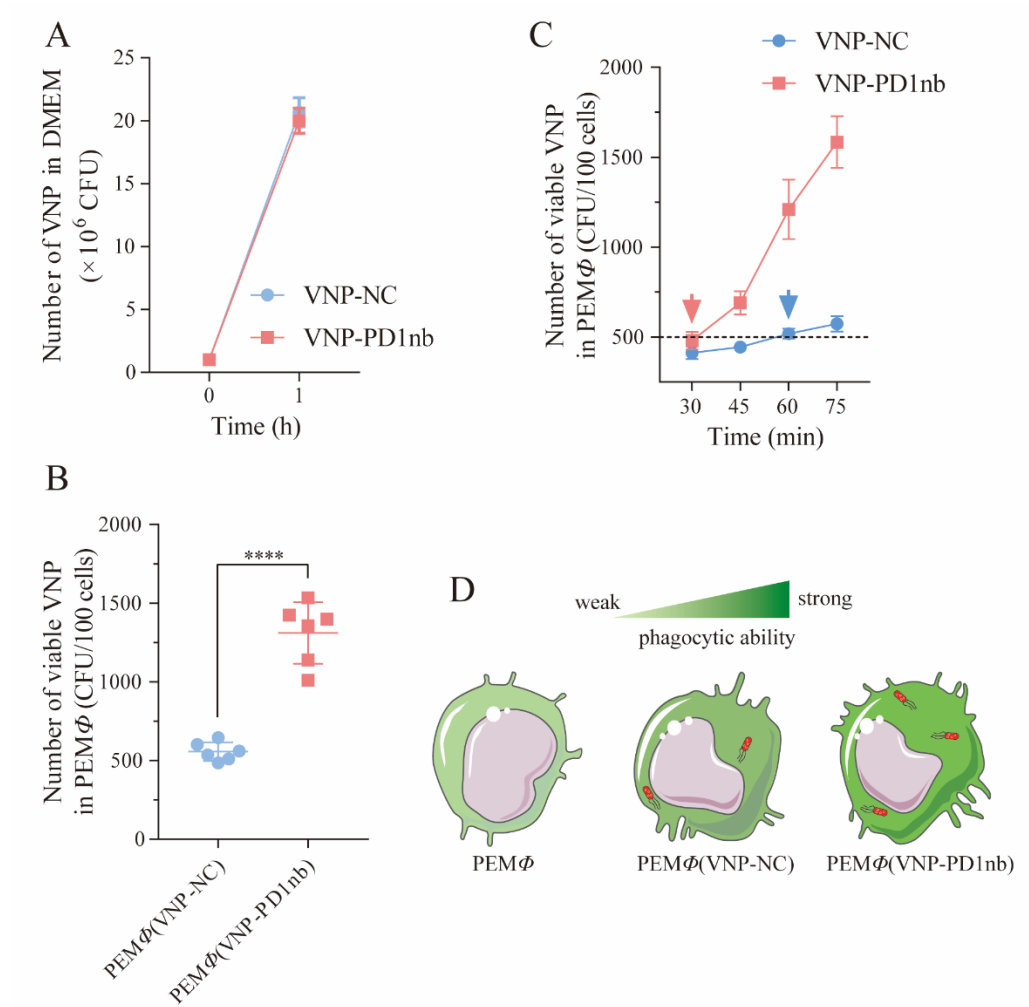


Figure S22 VNP-PD1nb enhances macrophage phagocytosis and leads to an increased VNP-loading capacity. (A) Comparison of the number of colonies between the VNP-NC and VNP-PD1nb groups after 1 h of culture in DMEM. (B) Quantification of viable intracellular VNP-NC or VNP-PD1nb strains after coculture with PEM Φ for 1 h at a ratio of 1:10. (C) The change curve of viable intracellular VNP-NC or VNP-PD1nb strains in the PEM Φ . (D) Schematic diagram of macrophage phagocytosis in different states. Data are reported as the mean \pm SEM. All data are representative of three independent experiments. Statistics were calculated using the two-tailed, unpaired Student's *t* test with Welch's correction. **** $P \leq 0.0001$.

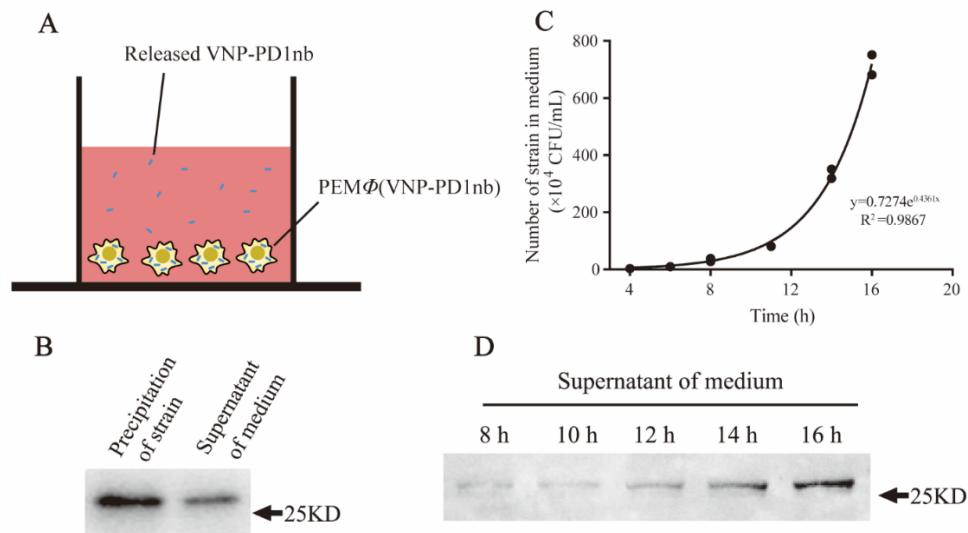


Figure S23 VNP-PD1nb can be released from macrophages and continuously secrete PD1nb. (A) The prepared PEM ϕ (VNP-PD1nb) cells were incubated in medium without antibiotics to release intracellular VNP-PD1nb, and the medium was collected at different times for subsequent experiments. (B) The medium collected at 14 h from (A) was centrifuged at 13,000 rpm for 10 min, and the total protein in the precipitate of the strain and the medium supernatant were collected by the method described in Section 2.16. The expression of PD1nb was analyzed by Western blotting. (C) The correlation between the number of VNP-PD1nb strains released from macrophages and the culture time in (A) was analyzed. (D) The secretion of PD1nb by the VNP-PD1nb strains released from macrophages at different time points in (C) (8–16 h) was detected by Western blotting. The medium supernatant was centrifuged to remove the bacteria, retaining only the secreted PD1nb. The protein was collected in equal volume (10 mL) of supernatant at different time points by trichloroacetic acid (TCA) precipitation, and 80 μ L of equal volume supernatant protein samples was obtained. The Western Blot assay results demonstrated the changes in PD1nb content in 15 μ L of samples over time.

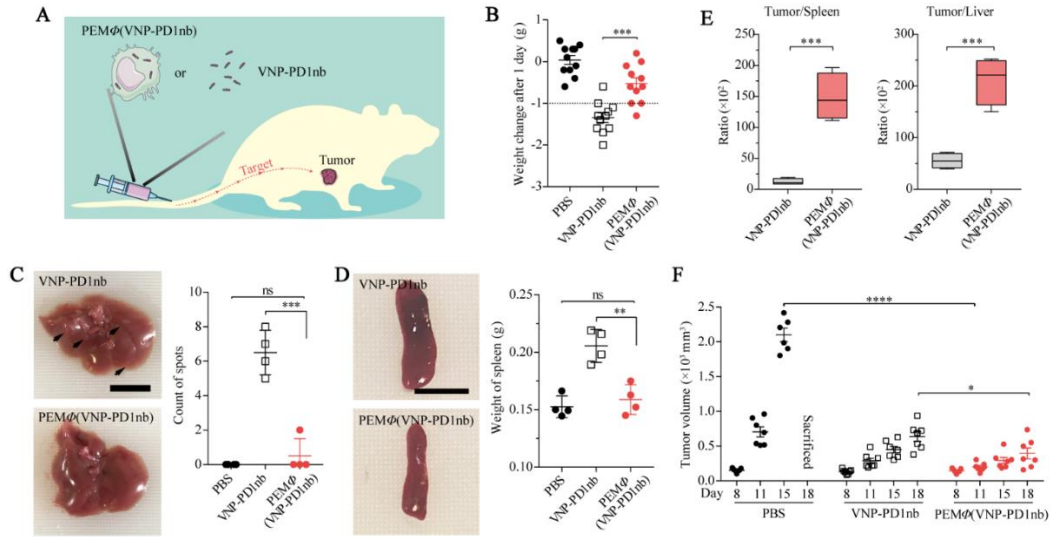


Figure S24 PEM Φ (VNP-PD1nb) cells effectively alleviate the side effects of VNP-PD1nb and inhibit tumor growth. (A) VNP-PD1nb and VNP-PD1nb-loaded PEM Φ (PEM Φ (VNP-PD1nb)) cells were administered *via* the tail vein, and their toxicities and tumor targeting were evaluated. (B) Changes in body weight 1 day after administration ($n = 11$ mice per group). (C) Photographs of representative livers. The black arrows indicate the pathological spots on the livers, and the numbers of spots are plotted in the chart (Scale bar = 10 mm). (D) Photographs of representative spleens. The weights of the spleens in each group are plotted in the chart (Scale bar = 10 mm). (E) The tumor:spleen (left) and tumor:liver (right) ratio of bacterial CFU per gram was calculated on the basis of recovered CFU from extracted organs on Day 6 ($n = 4$ mice per group in (C–E)). (F) Comparison of B16F10 tumor suppression in response to different treatments ($n = 7$ mice per group). “sacrificed” means that the mice were humanely sacrificed when the tumors reached an ethical limit. Data in (B–F) are reported as the mean \pm SEM. Boxplot representations of the spot counts. The median, interquartile range, and minimum and maximum identifiers are shown. All data are representative of two independent experiments. Statistics were calculated using the two-tailed, unpaired Student’s *t* test with Welch’s correction. n.s. = not significant, * $P \leq 0.05$, ** $P \leq 0.01$, *** $P \leq 0.001$, **** $P \leq 0.0001$.

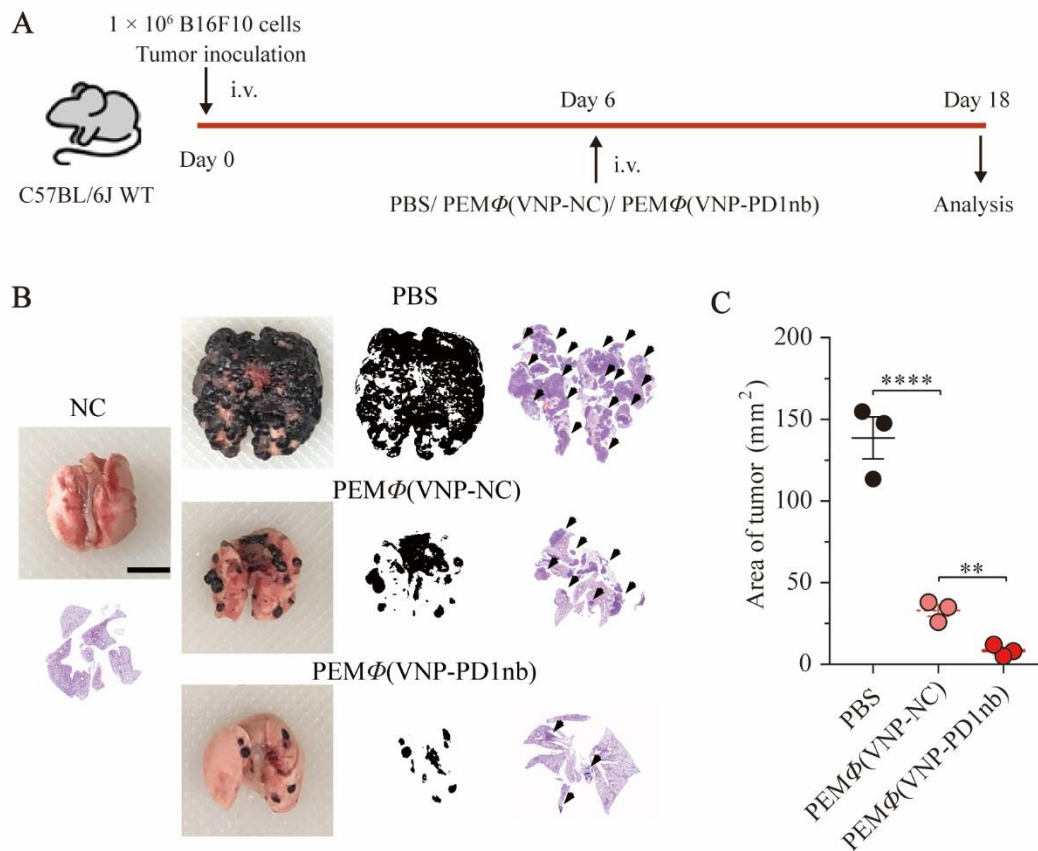


Figure S25 PEMφ(VNP-PD1nb) cells significantly inhibited the passive lung metastasis of melanoma. (A) Experimental scheme showing the treatment of the B16F10 lung metastasis C57BL/6J mouse model. (B, C) Comparison of the inhibitory effects of B16F10 on lung metastasis in the different groups. Representative images of H&E staining of lung sections are shown in (B), and the metastatic area is defined with a black arrow. ($n = 3$ mice per group, scale bar = 5 mm). ImageJ was used to analyze the tumor metastasis area, and the results are plotted in (C). Data are reported as the mean ± SEM. All data are representative of two independent experiments. Statistics were calculated using the two-tailed, unpaired Student's t test with Welch's correction. ** $P \leq 0.01$, **** $P \leq 0.0001$.

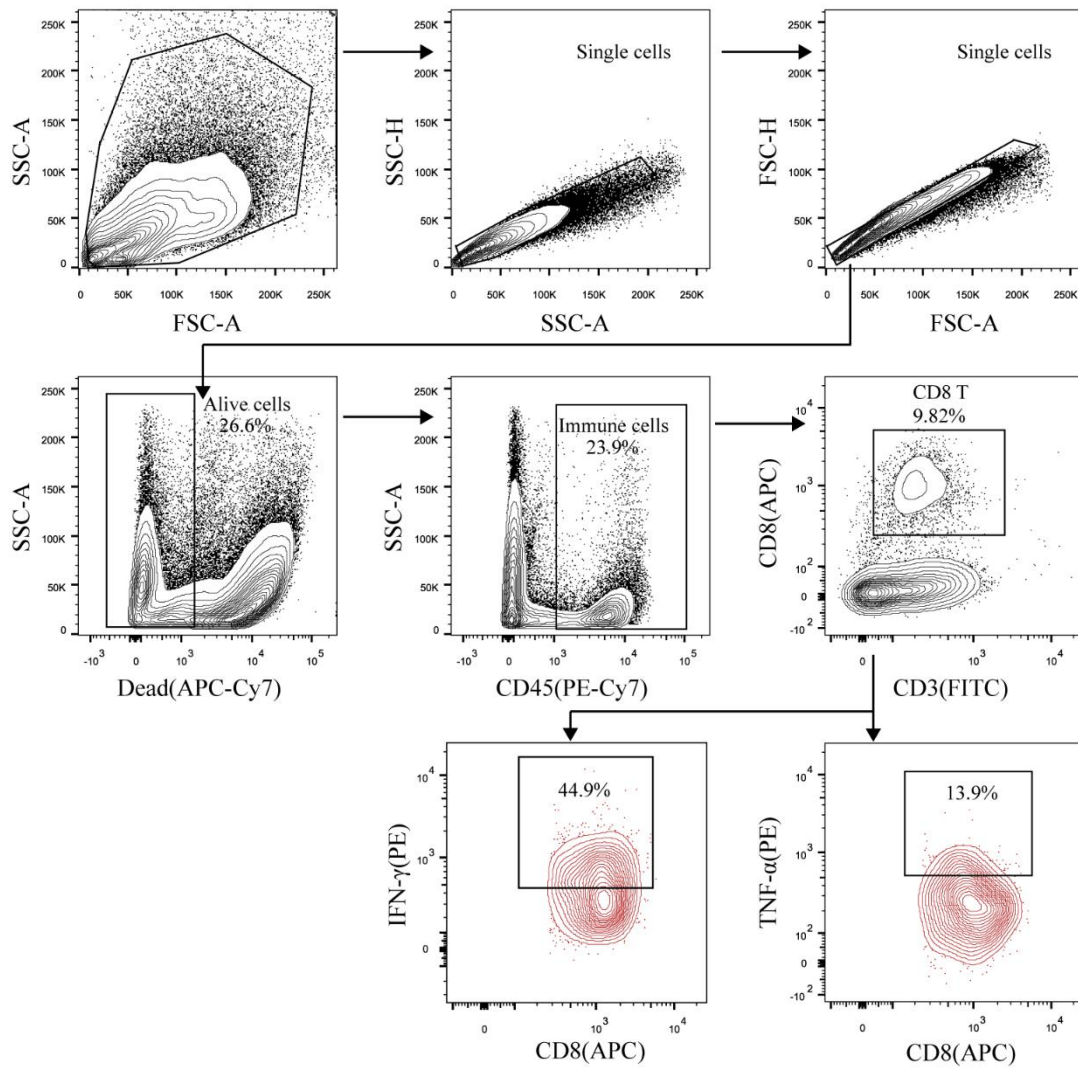


Figure S26 Representative gating strategy to identify CD8⁺ T cells producing IFN- γ and TNF- α .